

Study of temperature sensitive optical parameters and junction temperature determination of light-emitting diodes

Yue Lin, Yu-Lin Gao, Yi-Jun Lu, Li-Hong Zhu, Yong Zhang et al.

Citation: *Appl. Phys. Lett.* **100**, 202108 (2012); doi: 10.1063/1.4718612

View online: <http://dx.doi.org/10.1063/1.4718612>

View Table of Contents: <http://apl.aip.org/resource/1/APPLAB/v100/i20>

Published by the [American Institute of Physics](#).

Related Articles

Causes of driving voltage rise in phosphorescent organic light emitting devices during prolonged electrical driving
Appl. Phys. Lett. **101**, 173502 (2012)

Effect of diamond like carbon layer on heat dissipation and optoelectronic performance of vertical-type InGaN light emitting diodes
Appl. Phys. Lett. **101**, 171102 (2012)

A new model for optimization of organic light-emitting device by concurrent incorporation of electrical and optical simulations
J. Appl. Phys. **112**, 084507 (2012)

Hybrid white organic light-emitting diodes with a double light-emitting layer structure for high color-rendering index
J. Appl. Phys. **112**, 084504 (2012)

Improvement of optical performance of ZnO/GaN p-n junctions with an InGaN interlayer
Appl. Phys. Lett. **101**, 161905 (2012)

Additional information on *Appl. Phys. Lett.*

Journal Homepage: <http://apl.aip.org/>

Journal Information: http://apl.aip.org/about/about_the_journal

Top downloads: http://apl.aip.org/features/most_downloaded

Information for Authors: <http://apl.aip.org/authors>

ADVERTISEMENT

Universal charged-particle detector
for interdisciplinary applications:

- > Non-scanning Mass Spectrometry
- > Non-scanning Ion Mobility Spectrometry
- > Non-scanning Electron Spectroscopy
- > Direct microchannel plate readout
- > Thermal ion motion and mobility studies
- > Bio-molecular ion soft-landing profiling
- > Real-time beam current/shape tuning
- > Diagnostics tool for instrument design
- > Compact linear array for beam lines

Contact OI Analytical: +1-205-733-6900

The advertisement features a 3D perspective of a detector chip. A rainbow-colored arrow points from left to right across the top of the chip, with the text "Thermal hyper-thermal keV-energy ions Atmospheric Pressure to Ultra High Vacuum" written along its length. The chip itself is labeled "IonCCD™ for charged particles" in large, bold letters. Below this, it specifies "24µm spatial resolution (2136 pixels)" and "3ns temporal resolution (360 fps)". In the top right corner, the OI Analytical logo is displayed, consisting of the text "OI Analytical" next to a stylized globe icon.

Study of temperature sensitive optical parameters and junction temperature determination of light-emitting diodes

Yue Lin,¹ Yu-Lin Gao,¹ Yi-Jun Lu,^{1,a)} Li-Hong Zhu,¹ Yong Zhang,² and Zhong Chen^{1,b)}

¹Department of Electronic Science and Fujian Engineering Research Center for Solid-State Lighting, Xiamen University, Xiamen, Fujian 361005, People's Republic of China

²Electrical and Computer Engineering Department, University of North Carolina at Charlotte, Charlotte, North Carolina 28223, USA

(Received 11 December 2011; accepted 2 May 2012; published online 17 May 2012)

We investigate the current and temperature dependence of GaN-based high power blue light-emitting diodes and identify a set of temperature sensitive optical parameters (TSOPs) that can provide a real-time solution for determining the junction temperature (T_j). The relationships among T_j , forward current and TSOPs, “center of mass” wavelength, and, in particular, full width at half maximum (FWHM) have been studied, and the relevant mathematic models have been developed. The analysis indicates that using FWHM may yield higher accuracy than using other parameters as TSOPs. © 2012 American Institute of Physics. [<http://dx.doi.org/10.1063/1.4718612>]

In the past decade, a great deal of work has been devoted to improving properties and reliability of GaN-based light-emitting diodes (LEDs).^{1,2} The junction temperature (T_j) is an important device parameter that affects the performance, and it is directly related to the forward driving current (I_f). However, T_j usually cannot be directly measured under the operating condition. Therefore, an indirect measurement, relying on the dependence of one or more physical properties of the LED on T_j , is often adopted for the real-time monitoring of T_j . We show in Fig. 1 the typical dependence of the emission spectrum on T_j and I_f for a GaN based blue LED. With increasing T_j , the spectrum shows red-shift and broadening, whereas with increasing I_f the spectrum, instead, shows blue-shift and broadening. Although the detailed mechanisms of these phenomena are rather complex, the red-shift can be primarily attributed to the band gap reduction with increasing temperature³ and the blue-shift mainly to carrier screening effect as a result of increased injection current that weakens the piezoelectric field and thus the quantum confined Stark effect (QCSE).⁴ The I_f induced line width broadening is the combined effect of the screening to the piezoelectric field and band-filling. The former causes line width reduction, but the latter leads to line broadening.^{4,5} The T_j induced line width broadening is simply due to the thermal broadening effect.⁶

In this letter, we investigated the T_j and I_f dependences of the LED emission spectrum, and, based on the understanding of the above mentioned physical mechanisms, proposed a solution for the T_j real-time detection on GaN-based high power blue LEDs. The “center of mass” wavelength (λ_c) and full width at half maximum (FWHM) of the spectrum are chosen as the temperature sensitive optical parameters (TSOPs). λ_c is defined as

$$\lambda_c = \left(\sum_{\lambda=380\text{nm}}^{780\text{nm}} \lambda G(\lambda) \right) / \left(\sum_{\lambda=380\text{nm}}^{780\text{nm}} G(\lambda) \right), \quad (1)$$

where $G(\lambda)$ is spectral distribution. A model combining the T_j , TSOPs, and I_f is therefore established. Using this model, the real-time T_j of the LED under operating condition can be easily obtained by means of capturing the spectrum data. The measurements can be performed without changing or interrupting the voltage or I_f . Alternative methods have been proposed by Vaitonis⁷ and Bechou.⁸ They instead used the slope in a narrow spectral region of the high energy tail of the emission spectrum to determine the T_j for both AlGaInP and InGaN LEDs. The identification of the appropriate spectral range for this fitting is some extent subjective, and thus might affect greatly the accuracy.

As discussed above, the spectrum is affected by both I_f and T_j . Therefore, a function can be established to describe this relationship.

$$\sigma = f(T_j, I_f), \quad (2)$$

where σ is one of the TSOPs of the LED: for instance, λ_c or FWHM. The reason for choosing λ_c instead of the peak wavelength is that the former is determined from the whole spectrum rather than a single maximum point. It will be more immune to the noise in the low signal-to-noise ratio (SNR) cases compared to the peak wavelength.

The only way to extract the T_j from Eq. (2) is to find its function form. As discussed in the following sections, the TSOP- T_j relationship (at constant I_f) is linear, whereas the TSOP- I_f (at constant T_j) is exponential. Hence, it is better to determine initially the TSOP- T_j relationship, as revealed in Fig. 3. The slope k of the TSOPs vs T_j is nearly independent of I_f , which leads to

$$\partial\sigma/\partial T_j = k. \quad (3)$$

Integrating both sides, Eq. (3) leads to

$$\sigma = kT_j + C(I_f). \quad (4)$$

Since σ is a function of the I_f , the parameter C in Eq. (4) should also be I_f -dependent. In order to find the value of k

^{a)}Electronic mail: yjlu@xmu.edu.cn.

^{b)}Electronic mail: chen@xmu.edu.cn.

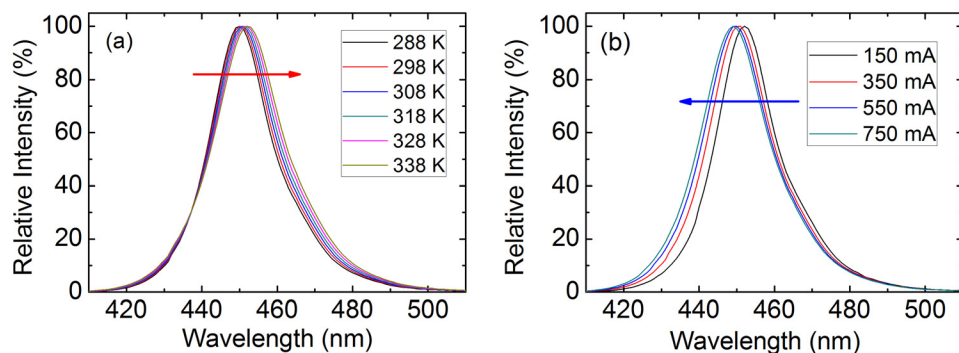


FIG. 1. (a) The temperature dependent red-shift when I_f was set at 350 mA, and heat sink temperature was varied from 288 to 338 K. (b) The I_f dependent blue-shift with the T_j set to 308 K.

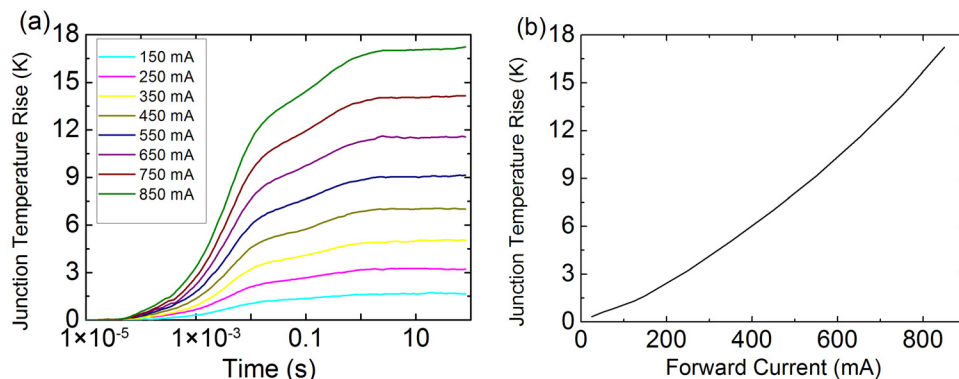


FIG. 2. (a) The ΔT_{jc} transient responses on each I_f on heat sink temperature set to 308 K. (b) The ΔT_{jc} - I_f relationship.

and the explicit expression of $C(I_f)$, we performed a two-step experiments as described below. The samples under this study are GaN-based 1 W blue LEDs with multiple quantum wells structures grown by metal organic chemical vapor deposition, manufactured by Cree Corp.

Step one: changing T_j , measuring σ , and calculating k with a series of I_f . The T_j was controlled by adjusting the heat sink temperature. Under a given I_f , even the heat sink temperature varies; the change in the junction-to-case temperature difference is insignificant. Therefore, the partial differential of σ with respect to T_j can be replaced by that to T_c (case temperature): $\partial\sigma/\partial T_j = \partial\sigma/\partial(T_c + \Delta T_{jc}) = \partial\sigma/\partial T_c = k$. The emission spectra were taken in the range of 380–780 nm. The I_f range was 150–850 mA with a 100 mA increment, and the temperature range of heat sink was 298–338 K with a 10 K increment.

Step two: obtaining the expression of $C(I_f)$ in Eq. (4). The T_j was kept at T_0 under a series of I_f from 150 to 850 mA with a 100 mA increment. Because of the strong self-heating effect,⁹ the I_f increase causes the surging of T_j . We measured the $\Delta T_{jc}(t)$ transient response under several I_f using a thermal transient tester (T3ster, Micred Corp.), as shown in Fig. 2(a), and made a ΔT_{jc} - I_f plot, which is illustrated in Fig. 2(b). The accuracy of the tester is ± 0.1 K. ΔT_{jc} is the junction-to-case temperature difference under each I_f . Thus, T_j can be maintained constant while varying the I_f by turning down heat sink temperature T_c by the corresponding ΔT_{jc} from T_0 according to Fig. 2(b). Specifically, we choose $T_0 = 308$ K in this experiment.

In the step one, linear regression is used to calculate the TSOP- T_j slopes for spectrums corresponding to different T_j with the same I_f . The results are illustrated in Fig. 3. Table I lists the 8 slopes of λ_c and FWHM as well as corresponding R-squares. All the R-squares are higher than 0.99, indicating

both λ_c and FWHM having a linear dependence on T_j . Since the slopes in all 8 currents are almost equal (8% maximum difference), the k value can be considered as current-independent, which indicates that temperature induced band-filling effect is barely affected by different injection current

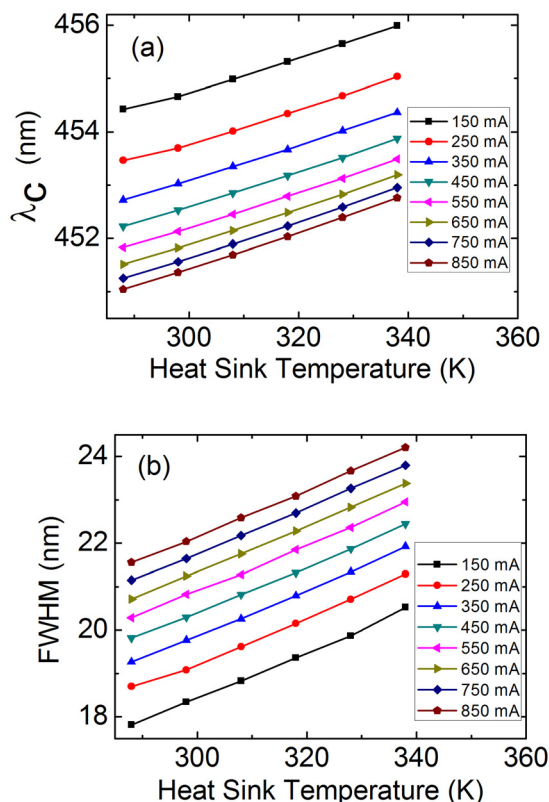
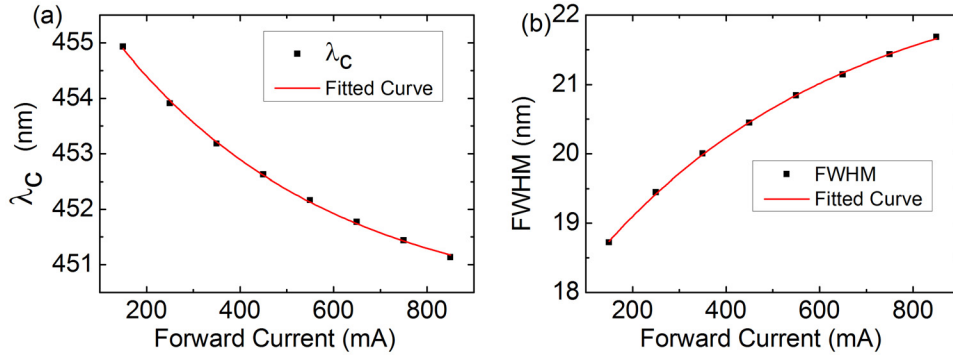


FIG. 3. The temperature dependent relationship of (a) λ_c and (b) FWHM on series I_f from 150 to 850 mA.

TABLE I. The slope and R-squares of the TSOP-temperature linear relationships on each forward current.

| I_f (mA) | | 150 | 250 | 350 | 450 | 550 | 650 | 750 | 850 |
|-------------------------|-------------|-------|-------|-------|-------|-------|-------|-------|-------|
| Slope (10^{-2} nm/K) | λ_c | 3.181 | 3.181 | 3.292 | 3.295 | 3.321 | 3.356 | 3.400 | 3.434 |
| | FWHM | 5.332 | 5.256 | 5.299 | 5.240 | 5.292 | 5.316 | 5.316 | 5.323 |
| R-square (10^{-1}) | λ_c | 9.970 | 9.960 | 9.993 | 9.992 | 9.991 | 9.992 | 9.991 | 9.992 |
| | FWHM | 9.979 | 9.966 | 9.990 | 9.991 | 9.989 | 9.998 | 9.996 | 9.993 |

FIG. 4. The I_f dependent relationship of (a) λ_c and (b) FWHM on the T_j set 308 K.TABLE II. Parameters and R-squares in the TSOP- I_f relationships.

| TSOPs | σ_0 (nm) | σ_1 (nm) | I_0 (mA) | R-square (10^{-1}) |
|-------------|-----------------|-----------------|------------|------------------------|
| λ_c | 450.15 | 6.58 | -458.43 | 9.989 |
| FWHM | 22.75 | -5.30 | -537.27 | 9.995 |

levels. In the following analyses, the slope of 350 mA is chosen. In the step two, the results are illustrated on Fig. 4, which indicates that the I_f increase leads to the monotonically decrease of λ_c with monotonically increase of FWHM. The slope become smaller when I_f is increased, revealing that the band-filling effect tends to be saturated with increasing I_f . The analytic expression of Eq. (5) is determined by curve fitting between σ and I_f .

$$\sigma|_{T_j=T_0} = kT_0 + C(I_f). \quad (5)$$

One-stage exponential function has enough accuracy (R-square > 0.99) to fit the data for both of the TSOPs (the curve on Fig. 4)

$$\sigma|_{T_j=T_0} = f_I(T_0, I_f) = \sigma_0 + \sigma_1 \exp(I_f/I_0), \quad (6)$$

where σ_0 , σ_1 , and I_0 are obtained from the least-square fitting, shown in Table II, as well as the R-Square values. Merging Eqs. (4)–(6), we obtain the expression of $C(I_f)$. The expression for σ can be described as follows:

$$\sigma = k(T_j - T_0) + \sigma_0 + \sigma_1 \exp(I_f/I_0). \quad (7)$$

TABLE III. Measuring results among two TSOPs model and forward-voltage method.

| I_f (mA) | | 150 | 250 | 350 | 450 | 550 | 650 | 750 | 850 | SD (K) |
|--------------------|-----------------|-------|-------|-------|-------|-------|-------|-------|-------|--------|
| Measured T_j (K) | Forward-voltage | 314.6 | 316.1 | 317.9 | 319.8 | 322.1 | 324.6 | 327.2 | 330.1 | N/A |
| | λ_c | 315.8 | 314.4 | 316.9 | 320.1 | 322.8 | 325.3 | 327.3 | 328.8 | 0.99 |
| | FWHM | 315.0 | 317.0 | 317.6 | 319.9 | 321.8 | 324.1 | 326.9 | 330.6 | 0.48 |

Rearranging Eq. (7), we have the final expression for T_j

$$T_j = [\sigma - \sigma_0 - \sigma_1 \exp(I_f/I_0)]/k + T_0. \quad (8)$$

Equation (8) can be used to test or monitor the T_j by substituting the TSOP (σ), I_f , and T_0 . Furthermore, if the spectrum can be measured at real time, the real-time T_j monitoring can be determined. In the future, the degradation effect^{10,11} should be taken into account to improve the long-term accuracy.

The T_j tested by the two TSOPs and forward-voltage method,¹² respectively, are listed in Table III for comparison. Under the same driving condition measured by forward-voltage method, those junction temperatures T_{0i} are used as references. The standard deviations (SDs) are given as follows:

$$SD = \sqrt{\sum_{i=1}^N (T_i - T_{0i})^2 / N}, \quad (9)$$

where N is the total number of times of measurements and T_i is the T_j measured by TSOP. In Table III, for certain currents, the error is larger in the λ_c model. Because of the larger R-square in the FWHM- I_f fitting, the SD of FWHM (0.48 K) is much lower than that of λ_c (0.99 K), revealing that FWHM as TSOP has a higher accuracy than λ_c .

In conclusion, we have investigated the temperature dependence of the emission spectrum in the GaN-based high power blue LED and extracted two TSOPs: λ_c and FWHM. We have found that on the case of GaN blue LED, the temperature-induced effect always shows a linear dependence

on T_j , whereas the current-induced effect shows an exponential dependence on I_f . A model has been developed to describe the dependence of T_j on λ_c and FWHM. The merit of this method is that a TSOP, rather than an electrical parameter, can be employed to the T_j measurement. Compared with the conventional forward-voltage method that inevitably interferes the working condition, the method proposed here is non-contact and does not affect the device operation.

This work at Xiamen University was supported in part by the Major Science and Technology Project between University-Industry Cooperation in Fujian Province under Grant No. 2011H6025, “863 Solid-State Lighting Project” of China under Grant No. 2006AA03A175, NSF project under Grant No. 11104230, and the NSF project of Fujian Province under Grant No. 2008J0030, at UNC-Charlotte partially by CRI.

- ¹Q. Z. Liu and S. S. Lau, *Solid-State Electron.* **42**, 677 (1998).
- ²M. A. Reshchikov and H. Morkoç, *J. Appl. Phys.* **97**, 061301 (2005).
- ³T. Wang, D. Nakagawa, J. Wang, T. Sugahara, and S. Sakai, *Appl. Phys. Lett.* **73**, 3571 (1998).
- ⁴L. Li, P. Li, Y. Wen, J. Wen, and Y. Zhu, *Appl. Phys. Lett.* **94**, 261103 (2009).
- ⁵J. Y. Zhang, L. E. Cai, B. P. Zhang, X. L. Hu, F. Jiang, J. Z. Yu, and Q. M. Wang, *Appl. Phys. Lett.* **95**, 161110 (2009).
- ⁶S. Chhajed, Y. Xi, Y.-L. Li, T. Gessmann, and E. F. Schubert, *J. Appl. Phys.* **97**, 054506 (2005).
- ⁷Z. Vaitonis, P. Vitta, and A. Žukauskas, *J. Appl. Phys.* **103**, 093110 (2008).
- ⁸L. Bechou, O. Rehioui, Y. Deshayes, O. Gilard, G. Quadri, and Y. Ousten, *Opt. Laser Technol.* **40**, 589 (2008).
- ⁹M. Kuball, S. Rajasingam, A. Sarua, M. J. Uren, T. Martin, B. T. Hughes, K. P. Hilton, and R. S. Balmer, *Appl. Phys. Lett.* **82**, 124 (2003).
- ¹⁰K. C. Yung, H. Liem, H. S. Choy, and W. K. Lun, *J. Appl. Phys.* **109**, 094509 (2011).
- ¹¹T. Yanagisawa and T. Kojima, *Microelectron. Reliab.* **43**, 977 (2003).
- ¹²Y. Lin, Y. J. Lu, Y. L. Gao, Y. L. Chen, and Z. Chen, *Thermochim. Acta* **520**, 105 (2010).